PROJECT ECHO

961-mc Lower-Sideband Up-Converter for Satellite-Tracking Radar

By M. UENOHARA and H. SEIDEL

(Manuscript received April 4, 1961)

A 961-mc lower-sideband up-converter has been specially designed to serve as preamplifier for the satellite-tracking radar used in Project Echo. The amplifier and its power supply are separately boxed and are installed directly behind the tracking antenna. The amplifier has been functioning most satisfactorily and has been used in routine manner to track the Echo satellite from horizon to horizon.*

This paper describes the design considerations, and details the special steps taken to ensure that the amplifier meets the particular system needs of low noise, absolute stability, insensitivity to temperature fluctuations, and high input-power level before onset of gain compression.

The satisfactory operation of this amplifier confirms the great potentiality of parametric amplifiers for stable, low-noise, high-frequency receivers.†

I. INTRODUCTION

The satellite-tracking radar amplifier operates at a center-band frequency of 961 mc in a lower-sideband mode and is pumped at 11.7 kmc; the output frequency of the amplifier is 10.739 kmc. The amplifier is unconditionally stable and its gain remains constant over long periods. The over-all noise figure of the amplifier, including the following mixer and IF stage, is less than 1.6 db; the gain at center band is 22 db and the bandwidth is 20 mc. The input power level that reduces the amplifier gain by 1 db is −26 dbm.

Since lower-sideband operation is employed, we are dealing with a regenerative amplifier, which is basically very sensitive to any changes

* Although this equipment was designed and constructed by the Bell System as part of its research and development program, it was operated in connection with Project Echo under Contract NASW-110 for the National Aeronautics and Space Administration.

† L. U. Kibler has come to similar conclusions in his paper[1] in this issue.

in circuit impedance and to fluctuations in the power supply. This feature has often been considered to be a disadvantage of parametric amplifiers in systems applications. To allay such fears, special precautions have been taken to stabilize the parametric amplifier. In particular, good isolators are provided to isolate the amplifier from any impedance fluctuations produced by antenna mismatches. Any fluctuation in the pump frequency is continuously corrected by an automatic frequency control, and all components, especially those near the diode, are made extremely rigid, thereby eliminating the possibility of impedance variations caused by mechanical vibrations. It is only through such careful design and engineering that the regenerative device can be, and indeed has been, made into a stable and reliable amplifier.

The system requirements of Project Echo made it necessary to pay special attention to the following two points:

(a) The amplifier had to be insensitive to large environmental changes; this was necessary because the amplifier was installed directly behind the antenna in order to reduce cabling losses. Otherwise, the insertion loss of the input circuit would degrade the noise performance of the system.

(b) The gain-compression characteristics had to be sufficiently good that, with an input power level of -26 dbm, the gain would be still within 1 db of the small-signal gain; at the same time, the over-all system noise figure had to be less than 1.8 db. This compression specification arose because the maximum possible leakage power from the 960-mc satellite communications transmitter was about -26 dbm at the radar receiver station.

It is difficult to construct a filter which has low insertion loss at 961 mc while suppressing a frequency only 1 mc away. If the gain compression were severe, with an input level of -26 dbm, the amplifier would be saturated by the leakage signal and the radar signal could not be detected. The power level at which compression sets in can be increased simply by decreasing the gain of the amplifier.* However, one must pay a penalty for decreasing the amplifier gain, since the over-all system noise figure increases through the increased noise contribution of the mixer and IF stages. The compression problem is thus not optimally solved simply by decreasing the amplifier gain; it requires a careful evaluation of the circuit design parameters.

The purpose of this paper is to describe the design consideration and the performance of the 961-mc amplifier with special emphasis on the

* For this particular amplifier the gain is almost constant until the output power reaches about -3 dbm. For example, for a gain of 22 db, the level at which compression sets in is about -25 dbm.

precautions taken to ensure that this amplifier met all the system requirements.

II. SPECIFICATIONS

The following were the specifications for the 961-mc preamplifier to be used with the Project Echo satellite-tracking radar:

Center-band frequency:	961 mc,
Over-all system noise figure:	<1.8 db,
Input power level at 960 mc for a gain compression of 1 db:	>-26 dbm.

The amplifier had to be unconditionally stable, providing constant gain over minimum periods of an hour. The amplifier also had to be installed as close as possible to the antenna to reduce the cabling loss from the antenna to the amplifier.

According to these specifications the amplifier was to be packed in a small box which would be mounted on the back of the parabolic dish. It was expected that the temperature of the environment of the amplifier would vary over a span of 80°F between midsummer and midwinter, and the performance of the amplifier had to be insensitive to such large environmental change. The amplifier had also to be insensitive to mechanical vibrations.

III. SELECTION OF MODE OF OPERATION

There are three presently accepted practical modes of operation of variable reactance communication amplifiers. They are all nondegenerate and are, respectively, the upper-sideband, the lower-sideband, and the reflection types. If ω_s is the signal frequency and ω_x is either the upper- or lower-sideband frequency, corresponding to either a positive or negative resistance device, then the minimum achievable system noise figures for uncooled systems are

$$F = 1 + \frac{\omega_s}{\omega_x}\frac{T_L}{290} \text{ (upper-sideband)},$$

$$F = 1 + \frac{\omega_s}{\omega_x} \text{ (lower-sideband or reflection)},$$

where T_L is the effective temperature of the load; that is, a fiction representing second-stage noise through the relationship

$$T_L = (F_2 - 1)\,290,$$

where F_2 is the noise figure of the second stage.

The formulae above assume the varactors to be totally noise-free and, further, that the negative-resistance modes may be operated at infinite gain. While neither assumption is to be taken too seriously, they permit, nevertheless, elimination of the upper-sideband device from major consideration. The load temperature T_L may be estimated by an optimistic assumption of 7 db for a mixer IF combination. Assuming a probable value of ω_s/ω_x of order one-tenth, then with no other consideration of noise sources, this term would account for about $1\frac{1}{2}$ db in its own right.

Both the lower-sideband and the reflection types of amplifier system have minimum excess temperatures operating at infinite gain condition. They provide identical noise figures and, at this gain, only the diode noise terms enter into account. This condition of infinite gain is evidently a singular one and corresponds, in principle, to the situation in which the diode regenerates its own losses as well as those of the idler-frequency cavity. Viewing the amplifier back from the idler port, it corresponds to a zero impedance source, and the idler load must correspondingly be decoupled infinitely if power is to be drawn from that source. It is little wonder, in the case of infinite gain, that the regeneration requirements of the lower-sideband amplifier require a higher order of infinity of regeneration than does the reflection type of device, and that it is by far the more unstable of the two.

As we drop down from the infinite gain condition, the negative source impedance rises from zero and the coupling coefficient to the load likewise rises from zero. The details of the noise sources within the load then become increasingly significant in determining over-all performance. The stability situation is ultimately reversed, in that the frequency-ratio gain available in the lower-sideband converter, in accounting for the second-stage noise, diminishes the need for regenerative gain over the reflection device, and the lower-sideband amplifier becomes more suitable for operation.

There were four reasons why a moderate gain was desired, in contrast to a very high gain, and which eventually made the lower-sideband converter the desired choice in system considerations for the Echo radar:

1. A reasonably wide bandwidth was desired to avoid frequency stability problems;
2. Too high a gain leads to compression problems;
3. Very large gain leads to pump stability problems;
4. Antenna mismatches require excessive isolation at high regenerative gain and noise is introduced through isolator forward loss.

In the selection of either the reflection or lower-sideband amplifier, the choice resided in the penalty paid to system noise performance for finite gain operation. The total system temperature is

$$T_{\text{syst}} = T_{\text{amp}}(G) + \frac{T_L}{G}.$$

In either amplifier type, T_L is typically of the order of 1200°K, and a gain of 20 db is thoroughly adequate to reduce second-stage noise. It may be shown that T_{amp} is well behaved as G decreases from infinity, and that the increase in system noise temperature from its minimum value is very nominal.

Assuming a 20-db amplifier gain, Fig. 1 shows (see Appendix A) that a choice of $R_L/R_S = 0.8$ (that actually employed) demands a regenera-

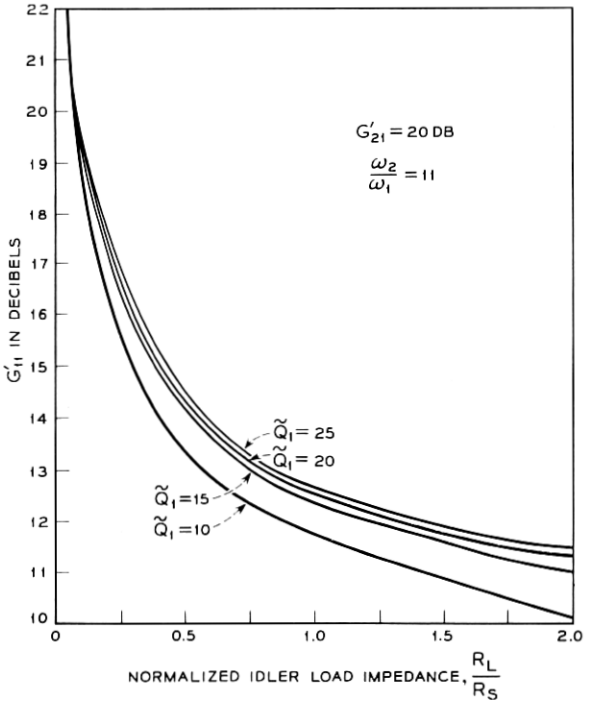

Fig. 1 — Regenerative gain G_{11}' of lower-sideband up-converter, which is needed to achieve a total gain G_{21}' of 20 db, vs. normalized idler load impedance R_L/R_S. The regenerative gains are shown for four different dynamic quality factors Q_1, with $Q_1 = 25, 20, 15$, and 10.

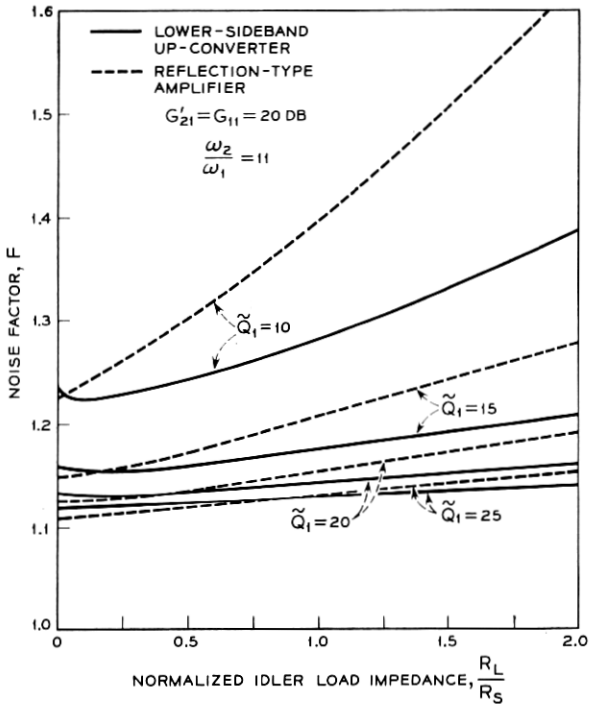

Fig. 2 — Noise figures of lower-sideband up-converter and reflection-type amplifier vs. normalized idler load resistance R_L/R_S . The curves for the lower sideband up-converter are shown by solid lines, those for the reflection type amplifier dashed lines. Gains are assumed to be the same at 20 db for both amplifiers.

tive gain of about 13 db for the lower-sideband amplifier, almost independently of $\tilde{Q}$,* in contrast to the 20 db for the reflection type. Further, as shown in Fig. 2, the lower-sideband noise figure (see Appendix B) at $R_L/R_S = 0.8$, at which it is trivially different from its minimum value, is significantly less than that for the reflection amplifier for $\tilde{Q}_1 < 25$. The parameters chosen in evaluating the curves of Figs. 1 and 2 are somewhat arbitrary, but are, nevertheless, typical for amplifiers of the type under consideration.

It was under the force of the above arguments, considering both stability and noise, that the lower-sideband amplifier was chosen in preference to the reflection type.

---

* The quality Q is defined in the next section and is a quality factor modified by the dynamic capacity ratio; R_L is the load impedance; and R_S is the diode-spreading resistance.

IV. VARACTOR DIODE SELECTION

There are two major requirements in the choice of a varactor diode:

1. It has to have an impedance sensible in magnitude to that of the generator.
2. It should have a high Q relative to its variable capacity portion.

The first requirement follows from the desire both to achieve reasonable bandwidth and to avoid large tuning losses in obtaining adequate interaction with the diode. The second follows from the fact that a static capacitor, however excellent its Q, cannot provide a basis for amplification, and its variability must be taken into account. A more realistic definition is given by[2]

$$\tilde{Q} = \frac{Q}{\frac{2C_0}{C_1} - \frac{C_1}{2C_0}},$$

where C_0 is the static capacitance at the operating point and C_1 is the capacitance associated with first dynamic term of the Fourier expansion of the time variable charge. The quantity Q is that value conventionally defined for the static capacitance, and is equal to

$$Q = \frac{1}{\omega C_0 R_s},$$

where R_s is the spreading resistance of the diode. This result assumes other loss mechanisms to be negligibly effective, which is given excellent confirmation experimentally.[3]

The choice of the value of C_0 is a most complex one if it is to be done correctly. Corresponding to a value of C_0 and its quality factor, there exist generator and load impedances which minimize noise. Transforming to these impedance levels requires tuning elements which are noise sources. Since the diode, as a waveguide scatterer, is an unknown from present analytic considerations, the computation of that value of C_0 which minimizes total system noise figure is not now achievable.

The actual selection of the static capacity value is intuitive and empirical. Since the capacitive impedance must be of the same order of magnitude as that of the generator, a first choice of C_0 is that in which

$$C_0 = \frac{1}{\omega_s R_g}.$$

This establishes the range of values of C_0, and initial experiments are performed to range in on an apparently best value. Experience has

demonstrated the choice to be fairly broad once a proper region has been found, since the tuning elements contribute but little loss.

The final question in choosing a diode relates to the material of the varactor. Diode development at this time has gone in two distinct directions in terms of the gallium arsenide point-contact and the silicon junction varactor. As of this writing, the gallium arsenide junction diode has shown no superiority over silicon, although it may yet well do so, and the selection was just between the aforementioned two.

The gallium arsenide point-contact diode has, to date, shown the highest achieved Q in practice, but has two mitigating features:

1. Currently available capacities are of order 0.5 $\mu\mu$f.
2. Its long-term reliability is not yet proven.

Under these circumstances it was deemed more advisable to choose a silicon junction varactor with a zero bias capacity of 3.5 $\mu\mu$f and a cutoff frequency of 70 kmc in contrast to double that frequency for the gallium arsenide diode. Measurement of the silicon varactor showed it to possess a value of $\bar{Q}$ of 22 at 960 mc, which is quite adequate for good performance.

V. DESCRIPTION OF THE AMPLIFIER

At the time this project was started, no suitable circulator was available at 960 mc. Of necessity, the choice was then that of the lower-sideband up-converter. However, even if a circulator had been available, the lower-sideband up-converter would still have been chosen for this particular application since it provides better stability, less severe compression, and possibly even better over-all noise performance, as discussed in the previous section.

The main features of the amplifier are as follows:

Input frequency, f_s :	961 mc,
Output (idler) frequency, f_i :	10.739 kmc (see Appendix C),
Pump frequency, f_p :	11.7 kmc,
Pump power supply:	TJ klystron (WE 455A) with AFC unit,
Bias voltage:	0 volt
$\frac{R_L}{R_s}$:	≈ 0.8
$\frac{R_g}{R_s}$:	≈ 22

Varactor diode:	silicon p-n junction diode in standard coaxial cartridge
f_c :	$\approx$70 kmc,
C_0 :	$\approx$3.5 $\mu\mu$f,
Estimated noise figure, F:	1.19 = 0.75 db (amplifier alone).

The reason for operating the diode at zero bias was to simplify the amplifier cavity structure through the absence of choking section, thereby improving stability. By doing this, a small sacrifice was made in the noise figure, since the dynamic quality factor decreases about 20 per cent, from $\tilde{Q} = 22$ to $\tilde{Q} = 17$, but the specifications were still met without any difficulty. The output circuit was designed to be near critical coupling under the no-pump condition. This coupling condition was also selected to improve the stability of the amplifier and the effects of compression.

One potential difficulty in employing a lower-sideband up-converter is the output frequency modulation due to fluctuation in the pump frequency. A slow frequency shift can, of course, be corrected by an AFC system. However, fluctuations which are fast and small cannot be corrected satisfactorily. This difficulty is solved by pumping the up-converter of the local frequency generator with the same pump supply as is used for the amplifier. The local oscillator consists of a lower-sideband up-converter and a 931-mc crystal-controlled modulator. The fluctuation of the 30-mc intermediate frequency is, therefore, exactly the same as that of the crystal oscillator.

A block diagram and photograph of the amplifier are shown in Figs. 3 and 4.

VI. CIRCUIT DESIGN

The first-order model of the parametric amplifier is well understood and accounts for the major portion of design. The parameters of this model may be found conveniently from a systematic static or "cold test" procedure,[3] which defines the central operating point and the pump swing. It determines a tuning and impedance-level loading procedure by identifying a static susceptance together with the first-order imaging effects produced by the pumping coupling of signal and image circuits.

The first-order theory oversimplifies somewhat and assumes a sinusoidal pump voltage swing of the diode, and also does not adequately account for the curvature of the charge voltage characteristic of the depletion layer. This latter effect greatly accentuates the charge drawn

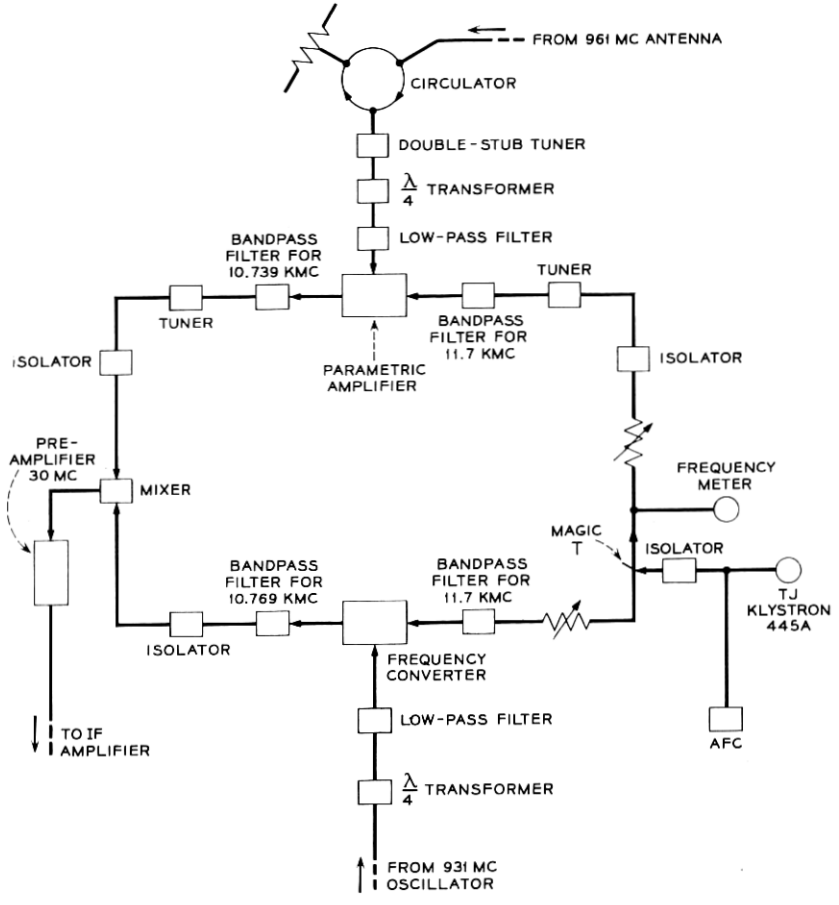

Fig. 3 — Block diagram of the 961-mc amplifier.

on the positive portions of the pump swing and increases the capacitive susceptance in viewing the system from either the signal or image port. The actual pump swing is defined in an equilibrium process of the pump, together with its complex network as a source, exciting the diode as a nonlinear element. Taking all things into account, the final tuning is completed by a dynamic or "hot" procedure.

The hot tuning may be accomplished adequately by a small bias increase to offset the effects of the pump excursion, and by a tuning touchup in the image circuit. This eliminates the need for variable tuning elements in the signal circuit where the effects of noise are major.

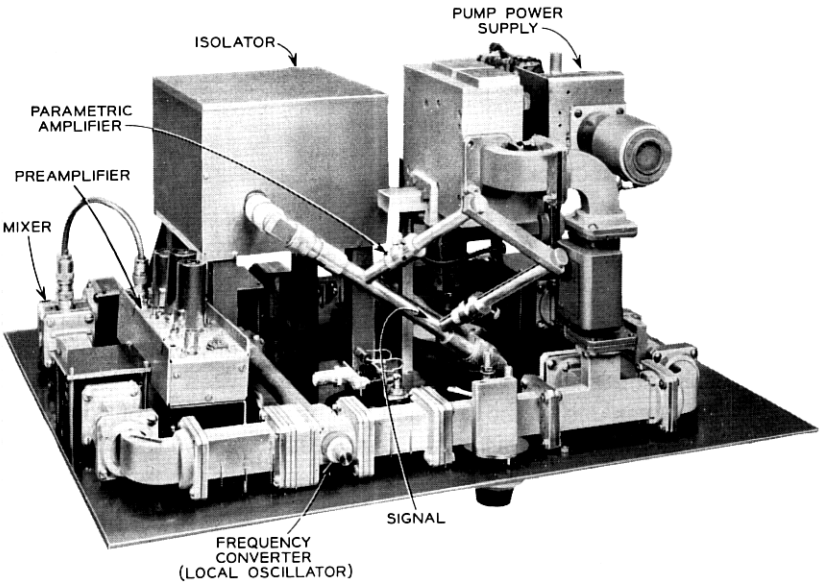

Fig. 4 — Photograph of the 961-mc amplifier.

The tuning procedure for minimum noise becomes increasingly difficult with high-Q elements, in that the spreading resistance of the diode is small and defies precise determination. Since the spreading resistance is the key to the impedance levels at signal and image frequencies, and since the effects of tuning losses become preponderant, the cold test procedure defers increasingly to the hot test with increasing Q. The demands on Q, however, are modest for most applications which do not demand ultimate noise performance, and the cold test procedure produces a good first design.

Tuning elements generally take the form of quarter-wave transformers, capacitive disks, and stubs. Final touchup is done by adjustable stub tuners in initial development. Figs. 3 and 4 show the early circuit for the Echo radar and still indicate the use of double stub tuners, but these were replaced by fixed elements in the final development.

The isolator is a most important unit in a stable parametric amplifier. It is desirable that the parametric amplifier system possess a large return loss. Since this number is typically 20 db, and since there is a return gain of the order of 13 db produced by regeneration, the isolator must possess a reverse loss of greater than 32 db, together with a minimal forward loss. The isolator must be stable to environmental cycling

so that its characteristics remain fixed. Small changes in the isolator are considerably amplified by the negative characteristics of the amplifier, and major consideration must be given both to mechanical and electrical stabilization.

VII. AMPLIFIER PERFORMANCE

The amplifier was designed as described in the previous sections. The general performance was satisfactory and closely approximated the design. The best measured over-all noise figure, including isolator, mixer, and IF amplifier, was 1.52 db with 22 db of gain and 20 mc of bandwidth; over-all noise figures of less than 1.6 db were obtainable without any difficulty. The noise figure of the amplifier portion itself was 1.33 db, of which 0.30 db was due to the insertion loss of the isolator, providing an inherent value of 1.03 db. This result is about 0.3 db above the theoretical value predicted for the diode, and suggests that the excess noise is probably caused by the tuner and the diode mount, and could be further reduced by careful engineering.

The stability of the amplifier was excellent. The gain varied by less than ± 1 db when the input impedance was varied from open-circuit to short-circuit. Under constant-temperature conditions, fluctuations in gain were mainly due to fluctuation in both pump frequency and pump power. The frequency problem was solved by using the electromechanical AFC, which was originally designed for the TJ radio relay system,[4] while the TJ klystron itself was already designed for extreme power stability. The electromechanical feature of the AFC tunes the klystron cavity without changing the output power, so that the combination of AFC system and TJ klystron greatly improves the stability of the amplifier.

VIII. TEMPERATURE DEPENDENCE OF AMPLIFIER GAIN

Experiment yielded relatively large irreversible temperature sensitivity in the initially constructed amplifier. This difficulty was ultimately traced to a resonance isolator at the amplifier input. It was found that the temperature variation

(a) varied the ferrite magnetization, shifting the resonant frequency slightly, and

(b) created a minor hysteresis loop in the magnetic structure, not returning the isolator to its initial state.

A circulator* was found to be somewhat less critically affected by temperature since, by its essential construction, it is not constrained to operate in the region of a narrow line width.

* Raytheon circulator CLL 8.

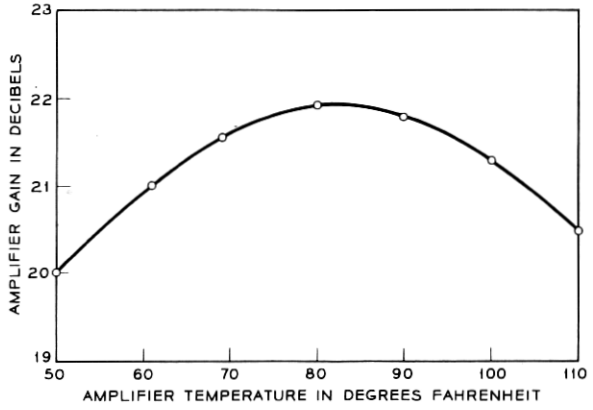

Fig. 5 — Amplifier gain vs. amplifier temperature.

Since the environmental variations seemed much beyond passive compensation, it was decided to thermostat the entire amplifier system at 110 ± 5°F and the circulator at 120 ± 2°F. The system incorporating this thermostating has demonstrated constant performance over a temperature range of 80°F.

Aside from the temperature sensitivity of the circulator, it was of interest to measure the temperature sensitivity of the amplifier section itself. Fig. 5 shows a 2-db variation at 20-db gain for ambient temperatures varying between 50 and 110°F. There is little sensitivity to be ascribed to the diode itself, and it must be presumed that this variation is due to expansion of circuit elements in critically tuned regions of the amplifiers.

Fig. 6 shows the noise figure of the amplifier section to be an exceedingly insensitive function of temperature over the range examined. In the measurements there was an initially deceptive appearance that the

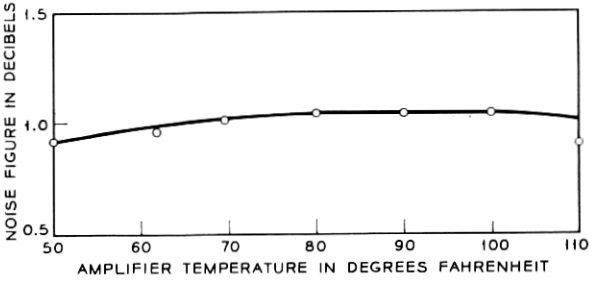

Fig. 6 — Noise figures vs. amplifier temperature.

noise figure increased much more rapidly than that in Fig. 6. This was shown, however, to be caused by the increased noise emission at higher temperature of the standard attenuators employed in conjunction with the measurements.

From the point of view of consistency, with the circulator thermostatting, the use of a 110°F ambient temperature for the amplifier to maintain gain stability provided no substantial noise-figure deterioration of the amplifier system.

IX. GAIN COMPRESSION

The Echo radar system was inherently complicated by the proximity of the 960-mc transmitter, just one megacycle away from the 961-mc radar frequency, which hit the amplifier at a level of −26 dbm. Engineering the amplifier to avoid compression was a major design requirement in the construction of the Echo radar system.

Compression occurs in a parametric amplifier system for any or all of the following reasons:

1. The circuit is detuned by the shift of the average capacity of the diode produced by the large signal swing;
2. Current is drawn on the positive swing in the forward direction and avalanche current exists on the negative swing;
3. The higher mixing products become significant compared to those of the small signal theory.

The source of compression is generally to be identified with the image circuit for two reasons:

1. The diode swing at image frequency exceeds that of the signal by virtue of the frequency ratio gain;
2. Minimum-noise operation implies high-Q image operation, where regeneration almost completely cancels cavity losses. This implies high-energy storage in the diode, with consequent large diode swing.

Compression may be mitigated at some slight expense to noise by increasing the image-circuit loading and consequently decreasing the image-cavity Q. The dynamic range may be further increased by reducing gain.

Naturally, there are limits, to which gain may be decreased or image loading increased, provided by the ultimately tolerable degradation of system noise figure. Employing the above considerations, the final amplifier design furnished a 22-db small-signal gain amplifier having a 1-db compression at an input of −26 dbm.

Another consideration in the presence of a high-level signal is the possibility of its inducing parasitic oscillations in the amplifier system.

Such parasitics were indeed noted and their presence was marked by very early onsets of compression. For want of any meaningful theory, these effects were eliminated empirically by small shifts of adjustment, which were apparently entirely successful in accomplishing this purpose.

X. LONG-TIME STABILITY

The gain of the amplifier was monitored over a period of 24 hours. A part of such a trace is shown in Fig. 7. The horizontal scale indicates time; the vertical scale gain. One vertical section corresponds to 0.5 db of gain variation. The gain shift over 24 hours was not more than ± 0.5 db out of 22 db. It is believed that these small fluctuations were caused primarily by power-line variation which affected an insufficiently regulated pump regulator supply used in the test.

XI. CONCLUSION

The design considerations and performance of the 961-mc lower-sideband up-converter have been discussed, and it has been emphasized that careful design and good engineering are necessary to obtain a stable low noise amplifier. An over-all system noise figure of less than 1.6 db has been obtained with a center-band gain of 22 db and a bandwidth of 20 mc. The amplifier is very stable, and the gain varies by less than ± 1 db as the input impedance is varied from open-circuit to short-circuit. With an input power of -26 dbm, the gain was 1 db less than the small signal gain of 22 db.

XII. ACKNOWLEDGMENTS

The design of this amplifier is very similar to that of an 860-mc amplifier designed at Bell Telephone Laboratories for a tropospheric communication system. The authors are greatly indebted to its various members who participated in this 860-mc project for transmitting to them their valuable experience, which added to the success of the present design.

P. J. Pantano did much of the mechanical design and the measurements. His ability and productive efforts during the entire period of this project are greatly appreciated. L. E. Cheesman helped this project during its early period. E. G. Spencer and W. A. Dean supplied the isolators and spent much effort to solve the temperature instability of the isolator characteristics. The author wishes to acknowledge their major contributions.

Acknowledgment is also made to K. D. Bowers for his stimulating

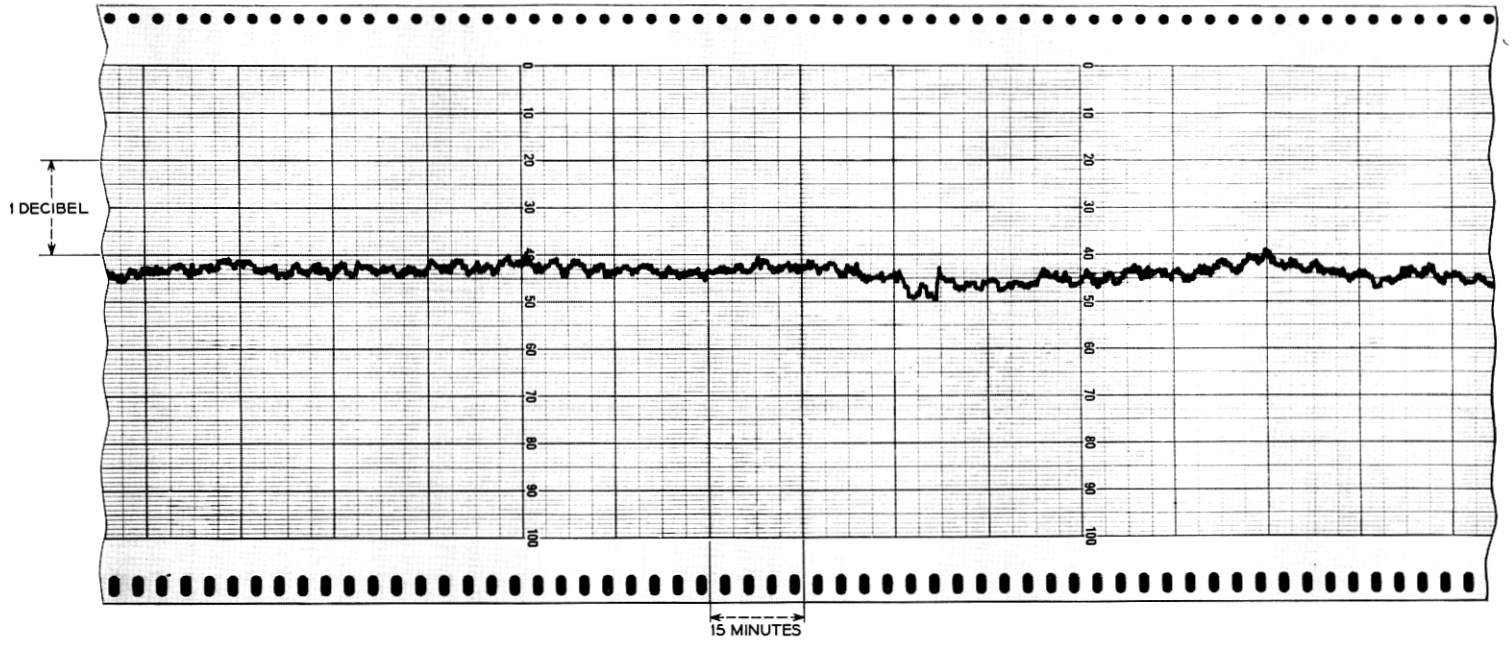

Fig. 7 — A part of a trace of the amplifier gain over a period of 24 hours. The gain shift over 24 hours was not more than ±0.5 db.

discussions and helpful criticism and encouragement in the study of this project.

APPENDIX A

Normalized Generator Impedance for Given Gain and Diode

The gain G_{11} of the reflection-type amplifier is given by the square of the voltage reflection coefficient[5] at the signal port, and is equal to

$$G_{11} = \frac{\left| \frac{Z_{11}^*}{R_S} - 1 + \frac{\tilde{Q}_1\tilde{Q}_2}{1 + \frac{Z_{22}^*}{R_S}} \right|^2}{\left| 1 + \frac{Z_{11}}{R_S} - \frac{\tilde{Q}_1\tilde{Q}_2}{1 + \frac{Z_{22}^*}{R_S}} \right|^2}, \tag{1}$$

and the gain G_{21}'* of the lower-sideband up-converter[2] is

$$G_{21}' = \frac{4 \frac{R_g'}{R_S} \frac{R_L'}{R_S} \tilde{Q}_1^2}{\left| \left(1 + \frac{Z_{11}'^*}{R_S}\right)\left(1 + \frac{Z_{22}'}{R_S}\right) - \tilde{Q}_1\tilde{Q}_2 \right|^2}. \tag{2}$$

Here Z_{11} and Z_{22} are the input circuit impedance and the idler circuit impedance, respectively, including the static capacitance of the diode; R_g, R_L, and R_S are the generator resistance, idler load resistance, and series resistance of the diode, respectively. At the center frequency, (1) and (2) can be simplified and become

$$G_{11} = \frac{\left[\left(\frac{R_g}{R_S} - 1\right)\left(1 + \frac{R_L}{R_S}\right) + \tilde{Q}_1\tilde{Q}_2\right]^2}{\left[\left(\frac{R_g}{R_S} + 1\right)\left(1 + \frac{R_L}{R_S}\right) - \tilde{Q}_1\tilde{Q}_2\right]^2}, \tag{3}$$

and

$$G_{21}' = \frac{4 \frac{R_g'}{R_S} \frac{R_L'}{R_S} \tilde{Q}_1\tilde{Q}_2 \frac{\omega_2}{\omega_1}}{\left[\left(\frac{R_g'}{R_S} + 1\right)\left(1 + \frac{R_L'}{R_S}\right) - \tilde{Q}_1\tilde{Q}_2\right]^2}, \tag{4}$$

* The notation associated with a lower-sideband up-converter will always be primed to indicate that the scattering properties of the network are not taken simultaneously with those of the reflection type, whose quantities will be left unprimed.

where ω_1 and ω_2 are the angular frequencies of the input and idler respectively, and the circuit losses are assumed to be negligible. Fluctuation in pump power alters $\tilde{Q}_1$ and $\tilde{Q}_2$, and, if the gain is reasonably high, fluctuation in $\tilde{Q}_1\tilde{Q}_2$ is equivalent to fluctuation in the circuit impedances R_g and R_L. At the same time, any fluctuation in the pump frequency adds reactive components to the circuit impedances. If the bandwidth of the amplifier is reasonably broad, small fluctuation in the pump frequency does not affect the gain of the amplifier significantly. The gain-bandwidth product is a simple measure of the stability of the amplifier to fluctuation in the pump frequency.

The most relevant measure of the stability of a parametric amplifier is the sensitivity of its gain to fluctuations in the resistance of the circuits. We shall now examine a measure of this sensitivity with the amplifier gain set at 20 db, a value close to that used in practice. The value of R_S/R_g is no longer coincident for both amplifier types. The major gain instability due to an impedance variation is caused by the denominators of (3) and (4), which are proportional to the regenerative gains of the amplifiers. To compare relative stability, therefore, it is much easier to compare the gain G_{11} of the reflection-type amplifier with the regenerative part G_{11}' (or input circuit gain) of the lower-sideband up-converter, whose total gain G_{21}' is equal to G_{11}. If G_{11}' is lower than G_{11}, the lower-sideband up-converter is the more stable, and vice versa. The values of R_g/R_S which provide gains G_{11} and G_{21}' for a given $\tilde{Q}_1$ and $\tilde{Q}_2$ are calculated from the following equations:

$$\begin{aligned}\frac{R_g}{R_S} &= \left(\frac{\tilde{Q}_1\tilde{Q}_2}{1+\frac{R_L}{R_S}}-1\right)\left[\frac{G_{11}+1}{G_{11}-1}+\sqrt{\left(\frac{G_{11}+1}{G_{11}-1}\right)^2-1}\right],\\ &= \left(\frac{\tilde{Q}_1\tilde{Q}_2}{1+\frac{R_L}{R_S}}-1\right)\left[\frac{(\sqrt{G_{11}}+1)^2}{G_{11}-1}\right],\end{aligned} \tag{5}$$

for the reflection-type amplifier, and

$$\begin{aligned}\frac{R_g'}{R_S} &= \left[\frac{2\frac{R_L'}{R_S}\tilde{Q}_1^2}{\left(1+\frac{R_L'}{R_S}\right)^2 G_{21}}+\frac{\tilde{Q}_1\tilde{Q}_2}{1+\frac{R_L'}{R_S}}-1\right]\\ &+\sqrt{\left[\frac{2\frac{R_L'}{R_S}\tilde{Q}_1^2}{\left(1+\frac{R_L'}{R_S}\right)^2 G_{21}}+\frac{\tilde{Q}_1\tilde{Q}_2}{1+\frac{R_L'}{R_S}}-1\right]^2-\left(\frac{\tilde{Q}_1\tilde{Q}_2}{1+\frac{R_L'}{R_S}}-1\right)^2}\end{aligned} \tag{6}$$

for the lower-sideband up-converter. The values of R_g/R_S which provide 20-db gain for given values of $\tilde{Q}_1$ and $\tilde{Q}_2$ are plotted as a function of R_L/R_S in Fig. 8. The dashed lines are those for the reflection-type amplifier and the solid lines are for the lower-sideband up-converter. Substituting the appropriate value of R_g/R_S for the lower-sideband up-converter into (4), one finds G_{11}'. The results are plotted in Fig. 2.

The load coupling factor for which G_{11} exceeds G_{21}' is determined by the condition

$$\left[\left(\frac{R_g'}{R_S} - 1\right)\left(1 + \frac{R_L'}{R_S}\right) + \tilde{Q}_1\tilde{Q}_2\right]^2 = 4\,\frac{R_g'}{R_S}\,\frac{R_L'}{R_S}\,\tilde{Q}_1\tilde{Q}_2\,\frac{\omega_2}{\omega_1}. \qquad (7)$$

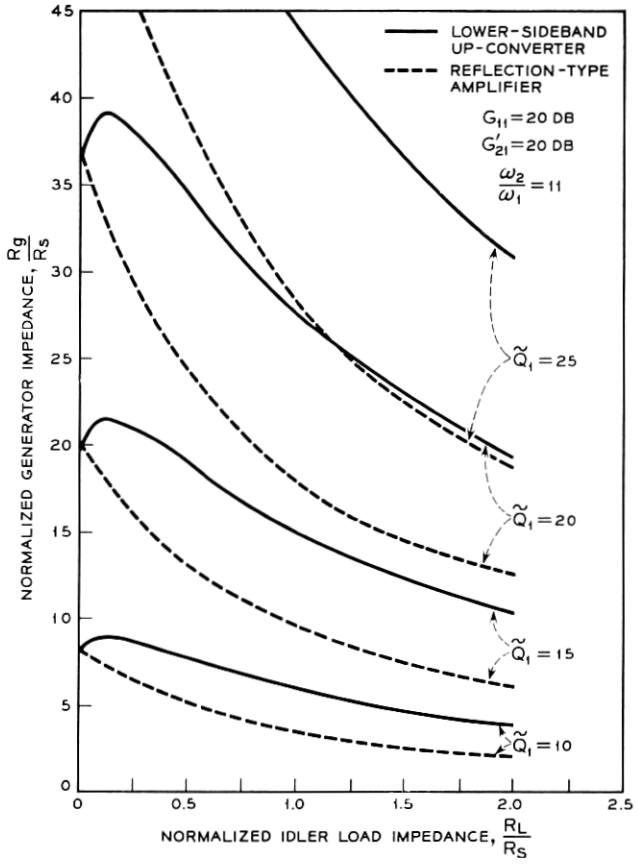

Fig. 8 — Normalized generator impedance R_g/R_S needed to obtain the gain of 20 db vs. normalized idler load impedance R_L/R_S . The curves for the lower-sideband up-converter are shown by solid lines; those for the reflection-type amplifier are shown by dashed lines.

A high-gain approximation leads to the simpler equation

$$\left(1 + \frac{R_L'}{R_S}\right)\frac{R_g'}{R_S} = \frac{R_L'}{R_S}\left(\frac{R_g'}{R_S} + 1\right)\frac{\omega_2}{\omega_1}, \tag{8}$$

from which R_L'/R_S is found to be

$$\begin{aligned}\frac{R_L'}{R_S} &= \frac{\omega_1}{\omega_2\left(1 + \dfrac{R_S}{R_g'}\right) - \omega_1} \\ &\approx \frac{\omega_1}{\omega_2 - \omega_1} \qquad \text{if} \qquad \frac{R_g'}{R_S} \gg 1.\end{aligned} \tag{9}$$

APPENDIX B

Noise Figure at Arbitrary Gain for Reflection-Type Amplifier and Lower-Sideband Up-Converter

The noise output of the reflection-type amplifier is

$$N_{\text{out}} = N_{11} + N_{12}, \tag{10}$$

where N_{11} is the noise output due to the noise sources in the signal circuit and N_{12} is the noise output due to those in the idler frequency circuit. The noise N_{11} contains two sources: one is the noise generated within the amplifier[2]

$$N = \frac{4\,KT\,B\,\dfrac{R_g}{R_S}}{\left[\left(\dfrac{R_g}{R_S} + 1\right) - \dfrac{\tilde{Q}_1\tilde{Q}_2}{1 + \dfrac{R_L}{R_S}}\right]^2}, \tag{11}$$

and the other is the input noise that is amplified

$$N = KT\,BG_{11}. \tag{12}$$

The noise N_{12} is given by[2]

$$N_{12} = \frac{4\,KT\,B\,\dfrac{R_g}{R_S}\,\dfrac{\tilde{Q}_1\tilde{Q}_2}{\left(\dfrac{R_L}{R_S} + 1\right)}\,\dfrac{\omega_1}{\omega_2}}{\left[\left(\dfrac{R_g}{R_S} + 1\right) - \dfrac{\tilde{Q}_1\tilde{Q}_2}{1 + \dfrac{R_L}{R_S}}\right]^2}. \tag{13}$$

From (10) through (13), the noise figure of the reflection-type amplifier is found to be

$$F = \frac{N_{11} + N_{12}}{KT\,BG_{11}}$$

$$= 1 + \frac{4\dfrac{R_g}{R_S}}{\left[\left(\dfrac{R_g}{R_S} - 1\right) + \dfrac{\tilde{Q}_1\tilde{Q}_2}{1 + \dfrac{R_L}{R_S}}\right]^2} + \frac{4\dfrac{R_g}{R_S}\dfrac{\omega_1}{\omega_2}\dfrac{\tilde{Q}_1\tilde{Q}_2}{1 + \dfrac{R_L}{R_S}}}{\left[\left(\dfrac{R_g}{R_S} - 1\right) + \dfrac{\tilde{Q}_1\tilde{Q}_2}{1 + \dfrac{R_L}{R_S}}\right]^2} \tag{14}$$

$$= 1 + \left(1 - \frac{1}{G_{11}}\right)\frac{1 + \dfrac{\omega_1}{\omega_2}\dfrac{\tilde{Q}_1\tilde{Q}_2}{1 + \dfrac{R_L}{R_S}}}{\dfrac{\tilde{Q}_1\tilde{Q}_2}{1 + \dfrac{R_L}{R_S}} - 1}.$$

Similarly, for the lower-sideband up-converter, the noise output is

$$N_{\text{out}} = N_{21} + N_{22}$$

$$= \frac{4\,KT\,B\left(\dfrac{R_g}{R_S} + 1\right)\dfrac{R_L}{R_S}\dfrac{\omega_2}{\omega_1}\dfrac{\tilde{Q}_1\tilde{Q}_2}{\left(\dfrac{R_g}{R_S} + 1\right)^2}}{\left[\left(\dfrac{R_L}{R_S} + 1\right) - \dfrac{\tilde{Q}_1\tilde{Q}_2}{\dfrac{R_g}{R_S} + 1}\right]^2} \tag{15}$$

$$+ \frac{4\,KT\,B\dfrac{R_L}{R_S}}{\left[\left(\dfrac{R_L}{R_S} + 1\right) - \dfrac{\tilde{Q}_1\tilde{Q}_2}{\dfrac{R_g}{R_S} + 1}\right]^2} + KT\,BG_{22},$$

where G_{22} is the reflection power gain of the idler circuit:

$$G_{22} = \frac{\left[\left(\dfrac{R_L}{R_S} - 1\right) + \dfrac{\tilde{Q}_1\tilde{Q}_2}{\dfrac{R_g}{R_S} + 1}\right]^2}{\left[\left(\dfrac{R_L}{R_S} + 1\right) - \dfrac{\tilde{Q}_1\tilde{Q}_2}{\dfrac{R_g}{R_S} + 1}\right]^2}. \tag{16}$$

Therefore, the noise figure of the lower-sideband up-converter is

$$F = 1 + \frac{R_S}{R_g} + \frac{1}{\frac{R_g}{R_S}\frac{\omega_2}{\omega_1}\frac{\tilde{Q}_1\tilde{Q}_2}{\left(\frac{R_g}{R_S}+1\right)^2}} + \frac{\left[\left(\frac{R_L}{R_S}-1\right)+\frac{\tilde{Q}_1\tilde{Q}_2}{\frac{R_g}{R_S}+1}\right]^2}{4\,\frac{R_g}{R_S}\frac{R_L}{R_S}\frac{\omega_2}{\omega_1}\frac{\tilde{Q}_1\tilde{Q}_2}{\left(\frac{R_g}{R_S}+1\right)^2}} \tag{17}$$

$$= 1 + \frac{R_S}{R_g} + \frac{\omega_1}{\omega_2}\left(\frac{\omega_2}{\omega_1}\frac{1}{G_{21}} + 1 + \frac{R_S}{R_g}\right)$$

$$= \left(1 + \frac{R_S}{R_g}\right)\left(1 + \frac{\omega_1}{\omega_2}\right) + \frac{1}{G_{21}}.$$

APPENDIX C

Optimum Idler Frequency for Arbitrary Idler Load

For high-gain and minimum-noise operation, the ratio of signal frequency to idler frequency is given by Equation (31) of Ref. 2. However, when R_L is not zero, the optimum idler frequency is different from that obtained using this equation, and it is instead determined by finding the value of ω_2 which minimizes the noise figure given by the following equation:

$$F = 1 + \frac{R_S}{R_g} + \frac{\left(\frac{R_L}{R_S}+1\right)R_S}{R_g}\frac{\omega_1}{\omega_2}\frac{\left(1+\frac{R_g}{R_S}\right)^2}{\tilde{Q}_1\tilde{Q}_2} \tag{18}$$

$$= \left(1 + \frac{R_S}{R_g}\right)\left(1 + \frac{\omega_1}{\omega_2}\right) + \frac{1}{G_{21}}.$$

Using the high-gain approximation of (6) for R_g/R_S as a function of frequency, we find

$$F = \left(1 + \frac{\omega_1}{\omega_2}\right)\left[1 + \frac{1}{\tilde{Q}_1^{\,2}\,\frac{\omega_1}{\omega_2}\,\frac{1}{1+\frac{R_L}{R_S}}}\right] + \frac{1}{G_{21}}. \tag{19}$$

Equation (19) leads readily to the result that

$$\frac{\omega_2}{\omega_1} = \frac{\tilde{Q}_1^{\,2}}{\left(1+\frac{R_L}{R_S}\right)\left(1+\sqrt{1+\frac{\tilde{Q}_1^{\,2}}{1+\frac{R_L}{R_S}}}\right)}. \tag{20}$$

The error in approximating the value of R_g/R_S at high gain is usually small, and provides negligible error in determining noise figure. Substituting the parameters given in Section V, ($R_L/R_S = 0.8$, $\tilde{Q}_1 = 17$), one finds that $\omega_2/\omega_1 = 11.7$. The optimum idler frequency is thus about 11.3 kmc. From this idler frequency the pump frequency is determined to be 12.261 kmc. Since the optimum frequency result leads to broad noise figure minima, it was decided to forego the exact pump frequency calculated in favor of one within the band of the Western Electric 445A klystron. This klystron, which has been designed for the TJ system, has a notably stable and long life. It was operated as a pump at the top of its range, at 11.7 kmc, producing an idler frequency of 10.739 kmc.

REFERENCES

1. Kibler, L. U., Standby Receiver System, this issue, p. 1129.
2. Kurokawa, K., and Uenohara, M., Minimum Noise Figure of the Variable-Capacitance Amplifier, B.S.T.J., **40,** 1961, p. 695.
3. Kurokawa, K., Theory of Cold Test of Variable-Capacitance Amplifier, to be published.
4. Gammie, J., and Hathaway, S. D., The TJ Radio Relay System, B.S.T.J., **39,** 1960, p. 821.
5. Uenohara, M., Noise Consideration of the Variable-Capacitance Parametric Amplifier, Proc. I.R.E., **48,** 1960, p. 169.